Demonstration of High-Order Dispersion Cancellation with an Ultrahigh-Efficiency Sum-Frequency Correlator

Joseph M. Lukens,[1] Amir Dezfooliyan,[1] Carsten Langrock,[2] Martin M. Fejer,[2] Daniel E. Leaird,[1] and Andrew M. Weiner[1,*]

[1]*School of Electrical and Computer Engineering, Purdue University, West Lafayette, Indiana 47907, USA*
[2]*E. L. Ginzton Laboratory, Stanford University, Stanford, California 94305, USA*

(Received 1 August 2013; published 7 November 2013)

We demonstrate dispersion cancellation of entangled photons for arbitrary spectral orders, generalizing Franson cancellation typically considered in second order alone. Employing ultrafast coincidence detection based on sum-frequency generation in a periodically poled lithium niobate waveguide with a record-high pair conversion efficiency of 10^{-5}, we verify cancellation of dispersion up to fifth order. Cancellation of odd-order phase is experimentally shown to require identical signal and idler dispersion coefficients, in contrast to even-order phase, which cancels with opposite signs. These results are especially important for future work on ultrabroadband biphotons.

DOI: 10.1103/PhysRevLett.111.193603 PACS numbers: 42.50.Dv, 42.65.Ky, 42.65.Lm, 42.65.Re

Group velocity dispersion, the variation of propagation velocity with optical frequency, plays a fundamental role in ultrafast optics [1]; methods to control and compensate it have proven essential in applications ranging from the generation of ultrashort pulses to optical communications. Such concerns naturally extend into the quantum regime as well, e.g., in the spreading of biphoton correlations [2] or heralded single-photon wave packets [3]. Yet the spectral correlation between entangled photons permits a *nonlocal* cancellation of this dispersion: the broadening of one photon can be completely undone by that of its entangled partner, leaving the biphoton correlation function unaltered even if the pair is arbitrarily far apart [4]. This cancellation was first observed on the femtosecond time scale [5] by employing ultrafast coincidence detection based on sum-frequency generation (SFG) [6–8].

However, such dispersion cancellation has been demonstrated for second-order spectral phase alone, whereas higher orders become increasingly important for wide bandwidths. The experimental examination of such effects is difficult with standard optical materials and components, due to the lack of independent control of each order, but is attainable with programmable Fourier transform pulse shaping [9], which has successfully been applied to entangled photons [10–12]. In typical pulse shapers [13], the input field is spectrally dispersed by a diffraction grating and made to impinge on an array of liquid crystal pixels; by controlling the voltage applied to each pixel, the phase of the corresponding Fourier component can then be programmed at will, thereby allowing for the creation of essentially arbitrary spectral filters, subject only to resolution constraints. In this work, by exploiting the flexibility permitted by a fine-resolution, fiber-pigtailed pulse shaper and a waveguide-based SFG correlator with orders of magnitude improvements in efficiency over past work, we succeed in demonstrating dispersion cancellation for arbitrary spectral orders. Our results are particularly relevant in the quest for single-cycle biphotons [14], as achieving band-limited correlation functions necessitates improved control of high-order spectral phase [15,16].

The entangled photons for our experiments are produced via spontaneous parametric down-conversion (SPDC) of a monochromatic pump laser. For a pump frequency of $2\omega_0$, the biphoton state can be calculated using perturbation theory [17] and is well expressed as

$$|\Psi\rangle = M|\mathrm{vac}\rangle_s|\mathrm{vac}\rangle_i + \int d\Omega\, \phi(\Omega)|\omega_0 + \Omega\rangle_s|\omega_0 - \Omega\rangle_i, \tag{1}$$

where $M \sim 1$, "vac" denotes the vacuum state, $\phi(\Omega)$ is a complex weight function determined by phase-matching conditions, and s and i represent signal and idler, respectively. The probability density for detecting an idler photon at time t and its corresponding signal at time $t + \tau$ is then proportional to the fourth-order (in field; second-order in intensity) correlation function $\Gamma^{(2,2)}(\tau)$, which can be expressed as the modulus squared of a biphoton wave packet $\psi(t + \tau, t)$ [18]

$$\psi(t + \tau, t) = \langle \mathrm{vac}|\hat{E}_s^{(+)}(t + \tau)\hat{E}_i^{(+)}(t)|\Psi\rangle, \tag{2}$$

where $\hat{E}_{s,i}^{(+)}(t)$ is the positive frequency electric field operator for the signal or idler, respectively. We have neglected the polarization and spatial degrees of freedom, which are unimportant in our experiments, and the stationarity of the photon source ensures that $\Gamma^{(2,2)}$ depends on τ only. If the photons propagate through separate linear and time-invariant systems before they are detected, the final wave packet, apart from a unimodular factor, is found to be

 © 2013 American Physical Society

$$\psi(t+\tau,t) \propto \int d\Omega\, \phi(\Omega) H_s(\omega_0+\Omega) H_i(\omega_0-\Omega) e^{-i\Omega\tau}, \tag{3}$$

where $H_{s,i}(\omega)$ is the spectral filter applied to the signal or idler, respectively. For lossless dispersive media described by general spectral phases $\Phi_{s,i}(\omega) = \sum_n \Phi_{s,i}^{(n)}(\omega-\omega_0)^n/n!$, the explicit form of the wave packet becomes

$$\psi(t+\tau,t) \propto \int d\Omega\, \phi(\Omega) \exp\Big\{-i\Omega\tau + i\sum_{n=0}^{\infty} \frac{1}{n!}[\Phi_s^{(n)} + (-1)^n \Phi_i^{(n)}]\Omega^n\Big\}. \tag{4}$$

Perfect dispersion cancellation, to all orders, is thereby obtained by the condition $\Phi_s^{(n)} + (-1)^n \Phi_i^{(n)} = 0$ for $n = 2, 3, 4, \ldots$.

It is interesting to note that the opposite sign of dispersion yields cancellation for even orders only; for odd orders, the *same* sign is required. The spectral anticorrelation of the entangled photons requires the signal and idler phases to be antisymmetric with respect to each other, i.e., that $\Phi_s(\omega_0+\Omega) = -\Phi_i(\omega_0-\Omega)$. Thus, odd-order coefficients must be matched, not flipped, for full cancellation. This condition is analogous to classical narrow-band SFG, which is sensitive only to the symmetric phase [19]. And this reveals a principal difference between Franson cancellation and dispersion insensitivity in Hong-Ou-Mandel (HOM) interference [20–22]. HOM dispersion cancellation places symmetry constraints only on the *total* biphoton phase, not on the particular functional forms of the signal and idler phases relative to each other. If we define $\Phi_T(\Omega) = \Phi_s(\omega_0+\Omega) + \Phi_i(\omega_0-\Omega)$, then the HOM interference pattern is unaffected so long as $\Phi_T(-\Omega) = \Phi_T(\Omega)$; i.e., the total biphoton phase must be a symmetric function of the signal frequency offset. Thus, the HOM interferometer is intrinsically insensitive to any even-order phase experienced by either photon [22], a property that has permitted narrow HOM dips even without true Franson cancellation [15,21]. On the other hand, the dispersion cancellation discussed in this Letter, which applies to the biphoton correlation function directly, demands the more stringent condition that the total biphoton phase be identically zero, for all orders above first.

In our experiments, we verify the generalized dispersion cancellation condition by considering each order independently, from $n = 2$ to 5. To do so, we employ a commercial pulse shaper (Finisar WaveShaper 1000S) based on liquid crystal on silicon technology, which features 10-GHz resolution from 191.250 to 196.275 THz—corresponding to 502 resolvable spectral regions. The only major drawback is its insertion loss of ~5 dB, and since we use SFG for detection, which scales quadratically with shared signal-idler optical loss [6,7], we thereby incur a 10-dB reduction in counts. However, as we show below, a high signal-to-noise ratio is still maintained by enlisting a periodically poled lithium niobate (PPLN) waveguide [23,24], which offers orders of magnitude improvements in nonlinear efficiency over bulk crystals [25].

The experimental setup is shown in Fig. 1. We couple a monochromatic pump laser at ~774 nm into the first 52-mm-long PPLN waveguide, which is temperature controlled to ~140°C. Entangled photons are generated around 1548 nm through degenerate down-conversion, for which we measure an internal efficiency of about 10^{-5} per coupled pump photon. The residual pump light is removed using three colored glass filters, and the generated SPDC photons are coupled into optical fiber. Because of the collinear, type-0 nature of the down-conversion process, it is impossible to distinguish signal and idler spatially or through polarization. Therefore, we define the signal photon as the member of the pair with frequency greater than ω_0 and the idler as its partner with frequency below ω_0, which allows us to independently control the spectral phase applied to each photon on a single pulse shaper [10,12]. The optical spectrum directly after the collimator is presented in Fig. 2(a), showing also the passbands for the signal and idler set by the pulse shaper; the total emission has a full width at half maximum of 8.25 THz. The entangled photons are subsequently manipulated either with dispersion-compensating fiber (DCF) or a pulse shaper and recombined through SFG in a second PPLN waveguide, temperature controlled to achieve a phase-matching curve spectrally aligned to the first. The remaining biphotons are then filtered out with more colored glass, and the SFG photons at 774 nm are detected on a silicon single-photon avalanche photodiode (PicoQuant τ-SPAD) with a dark count rate less than 20 s^{-1}. We choose the length of DCF to maximize the measured SFG count rate, finding that a link dispersion of −78 fs/nm optimally compensates the combined dispersion of the nonlinear crystals and the ~5 m of Corning SMF-28e fiber (with a nominal dispersion of

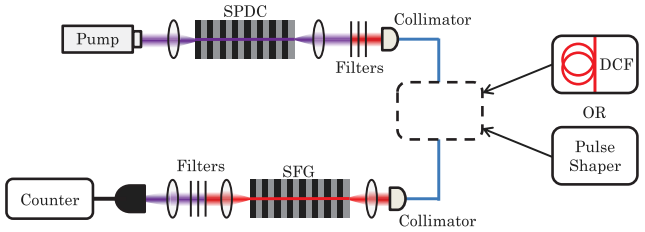

FIG. 1 (color online). Experimental setup. A continuous-wave pump laser at ~774 nm is coupled into the first waveguide, generating entangled photons around 1548 nm that are subsequently sent into optical fiber. Either DCF or a pulse shaper is used to manipulate the biphoton wave packet. Then the entangled photons are coupled into a second waveguide for up-conversion, and a single-photon counter detects the number of SFG photons at 774 nm. The second collimator and waveguide as well as the detector are housed in a box to exclude stray light.

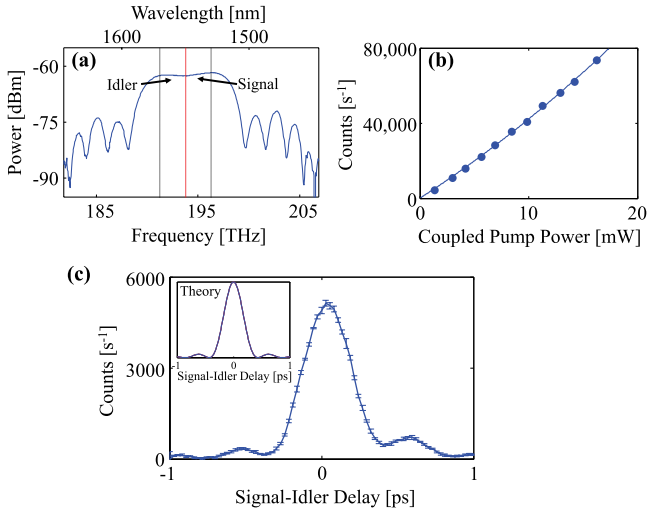

FIG. 2 (color online). Biphoton characterization. (a) Optical spectrum of generated SPDC photons, measured after the first collimator in Fig. 1 at 250-GHz resolution. (b) Detector counts as a function of power coupled into the first waveguide, when DCF is used. The log-log slope is 1.13. (c) Measured signal-idler temporal correlation function, with the pulse shaper used to achieve zero net dispersion. The theoretical result is given in the inset.

$\sim$16 fs/nm/m) used to connect the two PPLN waveguides across our optical table.

To verify that we are indeed operating in the isolated pair regime, we insert the -78-fs/nm DCF module described above and record the SFG counts as the pump is attenuated. In the multipair regime, the count rate is expected to scale quadratically, whereas a linear dependence is obtained for quantum light [6,7]. Figure 2(b) furnishes the results of this test. Each data point represents the average of five 1-s measurements, and the subtracted dark count rate is determined by recording the counts over 5 s when the pump is blocked. A log-log slope of 1.13 is found for the curve, confirming that we reside in the near-linear, quantum regime. The raw count rate is exceptionally high as well, reaching 74 100 s^{-1} at a coupled pump power of 16.3 mW. Accounting for losses between the two PPLN waveguides, the probability for a coupled photon pair to recombine in the second waveguide is found to be approximately 10^{-5}, comparable to our SPDC conversion efficiency and orders of magnitude higher than the 10^{-9} [12] or even 10^{-7} [6] reported in bulk media.

Such high efficiency allows us to endure the $\sim$10-dB reduction in counts introduced by the pulse shaper while still maintaining high count rates. Operating at the maximum power in Fig. 2(b), we replace the DCF with the pulse shaper, programming on it a baseline quadratic phase to achieve a net dispersion of zero and maximize SFG counts. Following the same procedure as in Ref. [10], the signal-idler correlation function is then obtained by sweeping through additional oppositely sloped linear phase terms applied to the signal and idler spectra and measuring the SFG counts at each step; the net signal-idler delay is proportional to the difference in these two slopes, thereby permitting tunable control of the relative photon timing. We note that, in general, SFG introduces distortions in the obtained correlation function due to phase-matching nonuniformity, as the up-conversion process actually filters the biphoton by its phase-matching curve [5,8]. However, our use of a pulse shaper restricts the SPDC bandwidth to within the nearly flat portion of the phase-matching response, ensuring that all frequency pairs combine freely. This produces an SFG flux directly proportional to $\Gamma^{(2,2)}(\tau)$, as we confirmed through simulation.

The result of our measurement is given in Fig. 2(c). Error bars depict the uncertainty in five 1-s measurements, after dark count subtraction. In this instance, we obtain the dark count rate by recording the counts when the pulse shaper is programmed to maximum (> 35 dB) attenuation, and this method is employed in all subsequent measurements. Even though the second waveguide and detector are isolated from ambient light by an enclosure, dark counts around 450 s^{-1} are found because of a monitoring light-emitting diode inside the shaper. The temporal FWHM of the correlation function is 370 fs, in good agreement with the 354 fs expected for a bandlimited flattop signal half-spectrum cut down to 2.5 THz by the pulse shaper. Simulations suggest that the slight asymmetry could be due to a small spectral mismatch between the phase-matching curves of the two crystals.

Defining the above applied phase as the zero point, for which the biphoton is approximately bandlimited, we add additional phase terms to examine the cancellation of arbitrary spectral orders. The particular phase coefficients are chosen to yield dispersed waveforms in the range of ± 5 ps, which is well within the ± 25-ps maximum delay possible with the pulse shaper. The second-order case is presented in Figs. 3(a) (theory) and 3(b) (experiment), for dispersion constants $\Phi_s^{(2)} = -\Phi_i^{(2)} = -0.3$ ps^2. With $\Phi_s^{(2)}$ applied to the signal, but nothing to the idler, a broadened correlation function is obtained; similar behavior is seen with nothing applied to the signal, but $\Phi_i^{(2)}$ on the idler. However, simultaneously applying both spectral phases returns the correlation function to its original, undispersed form, demonstrating complete cancellation. Proceeding to the next even order, with $\Phi_s^{(4)} = -\Phi_i^{(4)} = -0.01$ ps^4, we find the results of Figs. 3(c) and 3(d). Just as in the second-order case, fourth-order cancellation is obtained by applying the opposite sign of $\Phi_s^{(4)}$ to the idler, matching expected results from theory.

Odd-order spectral phase follows the reverse procedure, for the signal and idler expansion coefficients must be equal for cancellation to ensue. We verify this behavior for the third-order case in Figs. 4(a) and 4(b). Taking $\Phi_s^{(3)} = \Phi_i^{(3)} = -0.05$ ps^3, cancellation is indeed observed when the same third-order phase is applied to both signal

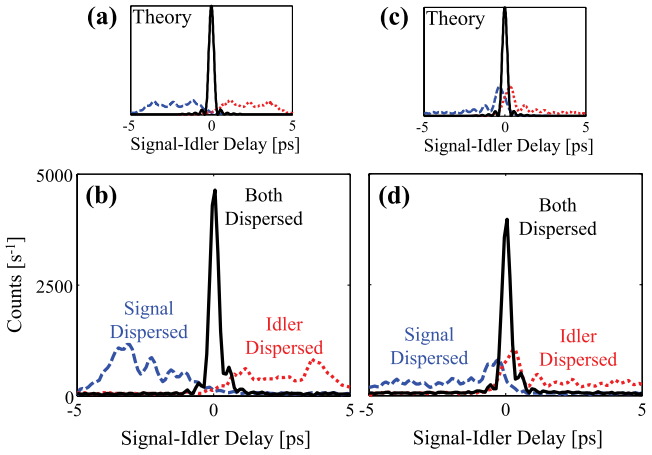

FIG. 3 (color online). Even-order dispersion cancellation. (a) Theoretical and (b) experimental results for second-order cancellation, using $\Phi_s^{(2)} = -\Phi_i^{(2)} = -0.3$ ps^2. Likewise, (c) theory and (d) experiment for fourth-order cancellation with $\Phi_s^{(4)} = -\Phi_i^{(4)} = -0.01$ ps^4. Error bars are omitted for clarity, but are comparable to those in Fig. 2(c), and each curve consists of 100 points spaced at 100 fs each. "Signal dispersed" and "idler dispersed" signify application of the specified phase to only one of the two photons, whereas "both dispersed" represents application to both.

and idler, even though broadening occurs in the individual cases. Finally, testing fifth-order phase with dispersion constants $\Phi_s^{(5)} = \Phi_i^{(5)} = -0.01$ ps^5, cancellation is again achieved, as shown in Figs. 4(c) and 4(d). The fact that even and odd orders carry opposite requirements highlights a crucial divergence from related dispersion effects with coherent or thermal optical sources. For example, in local dispersion compensation of classical pulses, all spectral orders in the compensating medium must be flipped relative to the dispersing medium. On the other hand, for dispersion cancellation with thermal light sources, the dispersion along both paths must be identical [26–28]. In either case, all spectral orders share a fixed cancellation condition, independent of parity, quite different from the alternating behavior shown here.

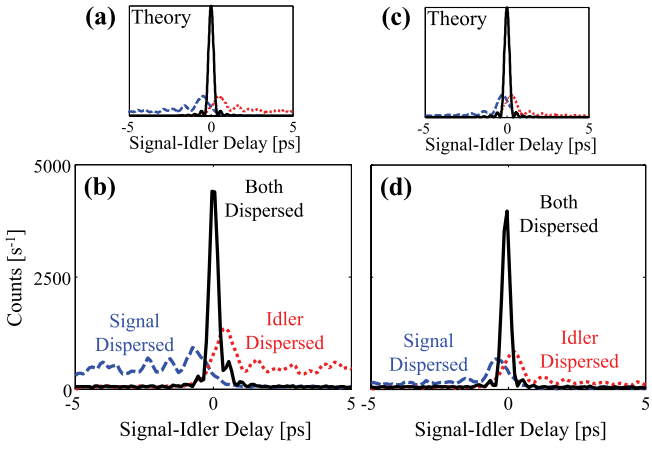

FIG. 4 (color online). Odd-order dispersion cancellation. Cancellation of third-order dispersion in (a) theory and (b) experiment, for the specific case of $\Phi_s^{(3)} = \Phi_i^{(3)} = -0.05$ ps^3. (c) Theoretical and (d) experimental cancellation of fifth-order dispersion, for $\Phi_s^{(5)} = \Phi_i^{(5)} = -0.01$ ps^5. The same considerations mentioned for Fig. 3 hold here as well.

In summary, we have implemented a waveguide-based ultrafast correlator for the measurement of the biphoton correlation function, featuring femtosecond resolution and vastly increased efficiency over the bulk crystals employed previously for such purposes. Inserting a fiber-pigtailed pulse shaper with programmable control of spectral amplitude and phase, we show dispersion cancellation of high spectral orders, from second to fifth. These results experimentally generalize Franson cancellation to all spectral phase functions that can be expressed as Taylor expansions. And in the future, by replacing the SFG waveguide and detector with fiber-coupled versions, our pulse shaper and correlator would no longer require free space optics, offering the potential for an entirely fiberized ultrafast biphoton correlator. Finally, although the timing resolution of most single-photon detectors [29] makes observation of these dispersive effects difficult for separated photons, up-conversion-assisted schemes with ultrafast gating [30,31] could be employed to show such dispersion cancellation without the need for biphoton recombination.

We thank V. Torres-Company for discussions. This work was funded by the Office of Naval Research under Grant No. N000141210488. J. M. L. acknowledges financial support from the Department of Defense through a National Defense Science and Engineering Graduate Fellowship.

*amw@purdue.edu

[1] A. M. Weiner, *Ultrafast Optics* (Wiley, Hoboken, NJ, 2009).
[2] A. Valencia, M. V. Chekhova, A. Trifonov, and Y. Shih, Phys. Rev. Lett. **88**, 183601 (2002).
[3] S.-Y. Baek, O. Kwon, and Y.-H. Kim, Phys. Rev. A **77**, 013829 (2008).
[4] J. D. Franson, Phys. Rev. A **45**, 3126 (1992).
[5] K. A. O'Donnell, Phys. Rev. Lett. **106**, 063601 (2011).
[6] B. Dayan, A. Pe'er, A. A. Friesem, and Y. Silberberg, Phys. Rev. Lett. **94**, 043602 (2005).
[7] B. Dayan, Phys. Rev. A **76**, 043813 (2007).
[8] K. A. O'Donnell and A. B. U'Ren, Phys. Rev. Lett. **103**, 123602 (2009).
[9] A. M. Weiner, Opt. Commun. **284**, 3669 (2011).
[10] A. Pe'er, B. Dayan, A. A. Friesem, and Y. Silberberg, Phys. Rev. Lett. **94**, 073601 (2005).
[11] B. Dayan, Y. Bromberg, I. Afek, and Y. Silberberg, Phys. Rev. A **75**, 043804 (2007).
[12] F. Zäh, M. Halder, and T. Feurer, Opt. Express **16**, 16452 (2008).
[13] A. M. Weiner, Rev. Sci. Instrum. **71**, 1929 (2000).
[14] S. E. Harris, Phys. Rev. Lett. **98**, 063602 (2007).

[15] M. B. Nasr, S. Carrasco, B. E. A. Saleh, A. V. Sergienko, M. C. Teich, J. P. Torres, L. Torner, D. S. Hum, and M. M. Fejer, Phys. Rev. Lett. **100**, 183601 (2008).
[16] S. Sensarn, G. Y. Yin, and S. E. Harris, Phys. Rev. Lett. **104**, 253602 (2010).
[17] L. Mandel and E. Wolf, *Optical Coherence and Quantum Optics* (Cambridge University Press, Cambridge, England, 1995).
[18] Y. Shih, Rep. Prog. Phys. **66**, 1009 (2003).
[19] Z. Zheng and A. M. Weiner, Opt. Lett. **25**, 984 (2000).
[20] A. M. Steinberg, P. G. Kwiat, and R. Y. Chiao, Phys. Rev. A **45**, 6659 (1992).
[21] A. M. Steinberg, P. G. Kwiat, and R. Y. Chiao, Phys. Rev. Lett. **68**, 2421 (1992).
[22] A. F. Abouraddy, M. B. Nasr, B. E. A. Saleh, A. V. Sergienko, and M. C. Teich, Phys. Rev. A **65**, 053817 (2002).
[23] K. R. Parameswaran, R. K. Route, J. R. Kurz, R. V. Roussev, M. M. Fejer, and M. Fujimura, Opt. Lett. **27**, 179 (2002).
[24] C. Langrock, S. Kumar, J. E. McGeehan, A. E. Willner, and M. M. Fejer, J. Lightwave Technol. **24**, 2579 (2006).
[25] S. Tanzilli, H. De Riedmatten, W. Tittel, H. Zbinden, P. Baldi, M. De Micheli, D. B. Ostrowsky, and N. Gisin, Electron. Lett. **37**, 26 (2001).
[26] V. Torres-Company, H. Lajunen, and A. T. Friberg, New J. Phys. **11**, 063041 (2009).
[27] V. Torres-Company, A. Valencia, M. Hendrych, and J. P. Torres, Phys. Rev. A **83**, 023824 (2011).
[28] V. Torres-Company, J. P. Torres, and A. T. Friberg, Phys. Rev. Lett. **109**, 243905 (2012).
[29] R. H. Hadfield, Nat. Photonics **3**, 696 (2009).
[30] O. Kuzucu, F. N. C. Wong, S. Kurimura, and S. Tovstonog, Opt. Lett. **33**, 2257 (2008).
[31] O. Kuzucu, F. N. C. Wong, S. Kurimura, and S. Tovstonog, Phys. Rev. Lett. **101**, 153602 (2008).